Physica Scripta. Vol. 40, 424–429, 1989.

Using Photon Correlation Spectroscopy to Study Small-Scale Turbulence

Walter I. Goldburg and Penger Tong

Department of Physics and Astronomy, University of Pittsburgh, Pittsburgh, PA 15260, U.S.A.

Abstract

The photon correlation spectroscopy technique was exploited to study turbulent pipe flow behind a grid. The correlation function of the scattered light intensity, $g(t)$, was found to be a scaling function of $qu(L)t(L_0/L)^\beta$ when the Reynolds number Re > 460. Here q is the scattering vector, L_0 the outer scale of the turbulent flow, and $u(L)$ is the characteristic turbulent eddy velocity associated with eddies of size L. The exponent β is a function of Re. The measurements of the half-decay time of $g(t)$ as a function of L and Re reveal an abrupt change in the character of the turbulent flow at Re = 460.

1. Introduction

A standard technique for studying laminar or turbulent flow is that of laser-Doppler velocimetry (LDV) [1, 2]. The flowing fluid is seeded with small particles which scatter the light while following local flow. The Doppler shifted light is mixed with the incident beam in a square-law detector, usually a photomultiplier. The detected signal then contains a component of the Doppler shift, $\boldsymbol{q} \cdot \boldsymbol{v}(\boldsymbol{r}, t)$, where $\boldsymbol{v}(\boldsymbol{r}, t)$ is the velocity of scatterers in the fluid. The scattering vector $\boldsymbol{q}$ has the amplitude $q = (4\pi n/\lambda) \sin(\theta/2)$, where θ is the scattering angle, n is the refractive index of the fluid, and λ is the wavelength of the incident light. This technique is especially useful for the case of laminar or weakly turbulent flow [3], where a single frequency $\boldsymbol{q} \cdot \boldsymbol{v}(\boldsymbol{r}, t)$ persists long enough to be measured.

For strongly turbulent flow it is more interesting to measure velocity differences rather than the local velocity $\boldsymbol{v}(\boldsymbol{r}, t)$. With a simple modification of the above LDV scheme, the difference $\boldsymbol{V}(\boldsymbol{R}, t) = \boldsymbol{v}(\boldsymbol{r}, t) - \boldsymbol{v}(\boldsymbol{r} + \boldsymbol{R}, t)$ is also measurable, as was demonstrated many years ago by Bourke *et al.* [4]. Here one records the intensity correlation function $g(t) = \langle I(t')\, I(t' + t)\rangle$, where $I(t)$ is the intensity of light falling on a photodetector. The technique yields information about velocity fluctuations without introducing an invasive probe, such as a hot wire anemometer [5]. Nor is it necessary to invoke Taylor's "frozen turbulence" assumption [6] to interpret the measurements. Intensity correlation spectroscopy has been especially fruitful in the study of diffusion motion of small particles in solution and molecular motion as well [7].

When the photon correlation technique is applied to the study of turbulence, one scatters and incident beam from seed particles, as in LDV, and $g(t)$ is the sum of terms, each of which contains the difference in Doppler shifts of particle pairs with velocity difference $\boldsymbol{V}(\boldsymbol{R}, t)$. As will be seen, $g(t)$ is simply related to the velocity distribution function, $P(\boldsymbol{V}(\boldsymbol{R}))$, that such a particle pair, separated by a distance $\boldsymbol{R}$, has velocity difference $\boldsymbol{V}(\boldsymbol{R}, t)$. More precisely, the measurement of $g(t)$ yields a weighted integral of the Fourier Cosine Transform of $P(\boldsymbol{V}(\boldsymbol{R}))$. By varying the direction of the scattering vector $\mathbf{q}$, one can measure the component of $\boldsymbol{V}(\boldsymbol{R}, t)$ in various directions with respect to the direction of mean flow.

In the theories of fully developed turbulence, the velocity difference $\boldsymbol{V}(\boldsymbol{R}, t)$ is expected to have self-similar character, i.e. the complete statistics of the velocity differences over varying length scales become identical under an appropriate scaling of velocity [8]. It is easy to show that the self-similar behavior of the moments of velocity difference can be obtained if the probability density function $P(\boldsymbol{V}(\boldsymbol{R}))$ has the scaling form $P(\boldsymbol{V}(\boldsymbol{R})/u(R))$, where $u(R)$ is a characteristic scaling velocity associated with size R. Theoretical models have been developed [9–11] and have led to predictions of self similarity of fully developed turbulence. Experiments at very large values of Re in air channels, ducts, and in the atmosphere confirm these predictions [12, 13].

Paralleling this research on strong turbulence, there have been recent developments in the theory of chaotic dynamics which provides a new paradigm for the understanding of the onset of turbulence [14]. The experiments described here are an investigation of turbulent flow between these two regimes.

We have exploited the photon correlation scheme to explore the small-scale turbulence at moderate Reynolds number in the familiar geometry of pipe flow through a grid [15] and find several notable features of the small-scale turbulence. At all but the smallest values of the Reynolds number Re, $g(t)$ obeys a scaling form, $g(t) = g(x)$, where

$$x = qu(L)t(L_0/L)^\beta. \tag{1.1}$$

Here L_0 is the outer scale of the turbulence which is proportional to the grid aperture size M, and $u(L) \sim (\varepsilon L)^{1/3}$ is the characteristic turbulent eddy velocity associated with eddies of size L. The exponent β turns out to be a function of Reynolds number Re. The parameter L is the width of a slit on which the scattered laser beam was focused. By varying the slit width one controls the size of the largest eddy and thus the largest velocity difference, $\boldsymbol{V}(\boldsymbol{R}, t)$, which contributes to the intensity $I(t)$ from which $g(t)$ is extracted with a standard photon correlator. As expected, the largest eddies have the largest velocity, so that a wide slit width implies a short decay time of $g(t)$. The fact that the argument x in eq. (1.1) is proportional to q rather than q^2, assures that $\boldsymbol{V}(\boldsymbol{R}, t)$ is not Gaussianly distributed and that one is not dealing with a diffusive phenomenon.

It will be seen in Section 2 that the factor $u(L)(L_0/L)^\beta$ in eq. (1.1) resembles the characteristic eddy velocity for fully developed intermittent turbulence even though we are far from this state. The maximum Reynolds number which can be reached in circulating water flow through a grid is much smaller than that which can be achieved in, say, an air channel, a jet, or in the open atmosphere. The exponent β appears in the theories of fully developed turbulence to characterize

its intermittent nature. Here β is not a function of Re. Experiments have provided approximate values for β through measurements of higher moments of the velocity fluctuations in the inertial range of spatial scales [12, 13]. In the Kolmogorov theory of fully developed turbulence [16], only two parameters are relevant, namely the kinematic viscosity ν of the fluid and the energy dissipation rate ε. At lower turbulent levels many parameters are presumably required to characterize the velocity field. We found, however, that in the range of $460 < \mathrm{Re} < 2500$, the scaling picture could still be applied to the velocity fluctuations, and the single additional parameter $\beta(\mathrm{Re})$ of eq. (1.1) sufficed to reduce $g(t)$ to scaling form for all values of the parameters L and q. By measuring how the half-decay time T of $g(t)$ depends on L, we extract the functional dependence of β on Re. The exponent β vs Re exhibits a kink at $\mathrm{Re} = 460$, suggesting the onset of the turbulent velocity distribution having scaling character. Near the maximum attainable value of Re, β has climbed to zero (Kolmogorov value). At the maximum accessible turbulent levels β begins to decrease, an indication that the turbulence begins to be intermittent.

It is useful to keep in mind the range of the controllable parameters in our experiment, and to compare them with relevant length and time scales of the fluid motion. The Reynolds number $\mathrm{Re} = MU/\nu$ could be varied from 31 to 3100 by adjusting the mean velocity, U, at the center of the pipe. Here ν is the kinematic viscosity which is $0.001\ \mathrm{cm^2\ s^{-1}}$ in water. The Kolmogorov dissipation length [16], $L_\mathrm{d} \simeq L_0(\mathrm{Re})^{-3/4}$, was of the order of 10 microns at $\mathrm{Re} = 3000$. Since this is much larger than the wavelength of light one could, in principle, reduce L well below L_d, in which case $u(L)$ would be constant over L, and the decay time of $g(t)$ may become independent of L. In practice we have not been able to focus the width of the laser beam below 0.1 mm.

From the correlation function $g(t)$ (glance ahead to Fig. 2), one gets a feeling for typical decay times; T was always less than 100 microseconds in our experiments. This characteristic time is much shorter than the turnover time of an eddy, $t_\mathrm{R} \sim R/u(R)$, which we estimate to be 10^{-3} s or more. Thus, in calculating $g(t)$ it may be assumed that each pair of seed particles separated by a distance $\boldsymbol{R}$ is moving at constant velocity, $\boldsymbol{V}(\boldsymbol{R}, t)$, in the time interval t of interest. This approximation will be made use of in relating the measured correlation function to the velocity distribution function $P(\boldsymbol{V}(\boldsymbol{R}))$.

It should be noted that even in the absence of flow, $g(t)$ will decay by virtue of the Brownian motion (diffusion) of the seed particles. With diffusion alone $g(t) \sim (1 + f(A) \exp(-2q^2Dt)$, where $f(A)$ is inversely proportional to the number of coherence areas viewed by the photodetector. The diffusivity D is inversely proportional to the radius of the diffusers. At $q = 2.42 \times 10^5\ \mathrm{cm^{-1}}$, corresponding to a scattering angle of 90°, $t_\mathrm{D} = (q^2D)^{-1} \approx 1 \times 10^{-4}$ s. Only in the laminar flow domain did diffusion compete with the flow fluctuations in limiting the decay time of $g(t)$. Even in the absence of both diffusion and turbulence, $g(t)$ will still decay in a finite time $T_\mathrm{u} \sim L/U$. This lifetime broadening effect was very small in our experiments, the measured decay time T being always at least a factor of 10 shorter than T_u.

When the scatterers move independently, as in diffusion, $g(t)$ can be factored into parts that depend on the spatial variables (for example, the angle subtended by the photodetector) and the dynamics [7]. In this case $g(t) = \mathrm{const} \times (1 + f(A)G(t))$. However when the particles move coherently, as in laminar flow for example, no such factorization is possible [17]. The turbulent situation would seem to lie between these two extremes, and empirically is was found that $g(t)$ could be factored as:

$$g(t) = \langle n\rangle^2(1 + f(L)G(t)), \tag{1.2}$$

where $\langle n\rangle$ is the average number of photon counts per sampling time and $f(L)$ is a spatial coherence factor.

The next section of this paper contains the derivation of the correlation function of the light intensity scattered by the particles in the turbulent fluid. Experimental details appear in Section 3, and the results are presented and analyzed in Section 4. Finally the work is summarized in Section 5.

2. Theory

The starting point is to consider the scattering produced by N identical particles suspended in a turbulent fluid. The diameter of the particles is taken to be small compared to the wavelength λ of incident light. In the simple case where the polarization of the incident beam is perpendicular to the scattering plane, the scattered electric field $E(t)$ is the sum of the fields radiated by each of the particles in the scattering volume, and has the form [4]

$$E(t) = \sum_j^N E_{sj}(t) = E_0 \exp(-\mathrm{i}\omega t) \times \sum_j^N \exp(-\mathrm{i}\boldsymbol{q} \cdot \boldsymbol{r}_j(t)). \tag{2.1}$$

Here $\boldsymbol{r}_j(t)$ is the trajectory of the jth particle relative to some origin inside the scattering volume, ω is the angular frequency of the incident light, and E_0 is an irrelevant proportionality factor involving the distance from source to detector, relative refractive index of the particles, and the wavelength λ.

The correlation function of the light intensity scattered by the particles in the turbulent fluid is, by definition,

$$g(t) = \langle \boldsymbol{E}^*(t')\boldsymbol{E}(t')\boldsymbol{E}^*(t' + t)\boldsymbol{E}(t' + t)\rangle / \langle \boldsymbol{E}^*(t')\boldsymbol{E}(t')\rangle^2 = K/Q^2. \tag{2.2}$$

Here

$$K = \left\langle \sum_{i,j,m,n}^N \exp\{\mathrm{i}\boldsymbol{q} \cdot [\boldsymbol{r}_j(t') - \boldsymbol{r}_i(t') + \boldsymbol{r}_m(t' + t) - \boldsymbol{r}_n(t' + t)]\} \right\rangle, \tag{2.3}$$

and

$$Q = \sum_{ij}^N \langle \exp\{\mathrm{i}\boldsymbol{q} \cdot (\boldsymbol{r}_j(t') - (\boldsymbol{r}_i(t'))\}\rangle = N + \sum_{i \neq j}^N \langle \exp\{\mathrm{i}\boldsymbol{q} \cdot (\boldsymbol{r}_j(t') - \boldsymbol{r}_i(t'))\}\rangle = N. \tag{2.4}$$

The fluctuation terms ($i \neq j$) do not survive a time or ensemble average if the scatterers are randomly distributed in the fluid.

Since the particles are assumed to follow the motion of the fluid, we have

$$\boldsymbol{r}_i(t' + t) = \boldsymbol{r}_i(t') + \int_{t'}^{t'+t} \mathrm{d}t''\, \boldsymbol{v}(\boldsymbol{r}_i(t''), t''), \tag{2.5}$$

where $\boldsymbol{v}(\boldsymbol{r}_i(t), t)$ is the flow velocity at position $\boldsymbol{r}_i$. Then

eq. (2.3) becomes

$$K = \sum_{i,j,m,n}^{N} \left\langle \exp\{i\boldsymbol{q} \cdot [\boldsymbol{r}_j(t') - \boldsymbol{r}_i(t') + \boldsymbol{r}_m(t') - \boldsymbol{r}_n(t')]\} \times \exp\left\{i\boldsymbol{q} \cdot \int_{t'}^{t'+t} dt''[\boldsymbol{v}(\boldsymbol{r}_m(t'')) - \boldsymbol{v}(\boldsymbol{r}_n(t''))]\right\}\right\rangle. \quad (2.6)$$

With the same assumption as we made for eq. (2.4), the fluctuation terms in eq. (2.6) may be dropped, and the remaining terms satisfy the condition,

$$\boldsymbol{r}_j(t) - \boldsymbol{r}_i(t) + \boldsymbol{r}_m(t) - \boldsymbol{r}_n(t) = 0, \quad (2.7)$$

when $q \neq 0$. The two possible choices to satisfy eq. (2.7) are $j = i, m = n, j \neq m$ and $j = n, m = i, m \neq n$. On dropping the inconsequential contribution from the term $i = j = m = n$, eq. (2.6) becomes,

$$K = N^2 + \sum_{m \neq n}^{N} \langle \exp\{i\boldsymbol{q} \cdot \boldsymbol{V}(\boldsymbol{R}(m, n), t')t\}\rangle = N^2 + 2\sum_{m>n}^{N} \langle \cos\{\boldsymbol{q} \cdot \boldsymbol{V}(\boldsymbol{R}(m, n), t')t\}\rangle, \quad (2.8)$$

and

$$g(t) = 1 + (2/N^2) \sum_{m>n}^{N} \langle \cos\{\boldsymbol{q} \cdot \boldsymbol{V}(\boldsymbol{R}(m, n), t')t\}\rangle. \quad (2.9)$$

Here $\boldsymbol{V}(R(m, n), t) = \boldsymbol{v}(\boldsymbol{r}_m, t) - \boldsymbol{v}(\boldsymbol{r}_m + \boldsymbol{R}(m, n), t)$, $\boldsymbol{R}(m, n) = \boldsymbol{r}_n(t) - \boldsymbol{r}_m(t)$, and the integral in eq. (2.6) is replaced by $\boldsymbol{V}(\boldsymbol{R}(m, n), t) \times t$ because the turbulent eddy turnover time, $t_R \sim R/u(R)$, is much longer than the delay times t of interest in our experiment.

When $N \gg 1$, the summation in eq. (2.9) can be converted into an integration over the scattering volume. Therefore eq. (2.9) becomes [18]

$$g(t) = 1 + \int_0^L dR\, h(R) \langle \cos\{\boldsymbol{q} \cdot \boldsymbol{V}(\boldsymbol{R}, t')t\}\rangle. \quad (2.10)$$

Here the scattering volume is assumed to be quasi-one dimensional with length L, and $h(R)$ is the number distribution of particle pairs separated by distance R in the scattering volume. When N particles are evenly distributed in a one-dimensional scattering volume with length L, the fraction of particle pairs separated by R is

$$h(R) = (N - n)/(N(N - 1)/2) \simeq (2/N)(1 - n/N) = (2/L)(1 - R/L). \quad (2.11)$$

If we assume the ensemble average of the turbulent velocity distribution is equivalent to the time average, eq (2.10) may be written in an alternative form

$$g(t) = 1 + \int_0^L dR\, h(R) \times \int_{-\infty}^{\infty} dV_q(R)\, P(V_q(R) \cos\{qV_q(R)t\}, \quad (2.12)$$

where $V_q(R)$ is the component of $V(R)$ along $\boldsymbol{q}$. If the turbulence is isotropic $P(V_q(R))$ is independent of $\boldsymbol{q}$.

If $P(V_q(R))$ is assumed to have the scaling form

$$P(V_q(R)) = u(R)^{-1}\, Q(V_q(R)/u(R)), \quad (2.13)$$

where $u(R)$ is a characteristic scaling velocity. Then eq (2.12) becomes

$$g(t) = 1 + \int_0^L dR\, h(R) \int_{-\infty}^{\infty} d(V_q(R)/u(R)) \times Q\{V_q(R)/u(R)\} \cos\{qu(R)t\, V_q(R)/u(R)\} = 1 + \int_0^L dR\, h(R)\, F(qu(R)t), \quad (2.14)$$

where $F(qu(R)t)$ is the Fourier Cosine Transform of the velocity distribution function $Q(V_q(R)/u(R))$.

The Kolmogorov theory of fully developed isotropic turbulence [16] gives

$$\langle V(R, t)^n\rangle = B_n \langle V(R, t)^2\rangle^{n/2}, \quad (2.15)$$

where B_n are apparatus-independent constants and $V(R, t)$ is the amplitude of $V(R, t)$. Equation (2.15) applies to separation R is in the inertial range $L_d \ll R \ll L_0$, where L_d is the Kolmogorov dissipation length and L_0 is the outer scale of turbulence. Using eq. (2.13), we have

$$\langle V(R, t)^n\rangle = \int_{-\infty}^{\infty} d(V(R)/u(R))\, Q\{V(R)/u(R)\}\, V(R)^n = B_n u(R)^n, \quad (2.16)$$

where

$$B_n = \int_{-\infty}^{\infty} dz\, Q(z)\, z^n. \quad (2.17)$$

So according to the Kolmogorov picture the characteristic scaling velocity $u(R)$ in eq. (2.13) is

$$u(R) = \langle V(R, t)^2\rangle^{1/2} \sim (\varepsilon R)^{1/3}, \quad (2.18)$$

where ε is the energy dissipation rate of turbulent flow.

Taking the intermittency of turbulence into account, the β-model predicts [8] that

$$\langle V(R, t)^n\rangle = B_n(\varepsilon R)^{n/3}(R/L_0)^{\beta(3-n)}, \quad (2.19)$$

with $\beta = (d - D)/3$, where d is the imbedding dimension, and D is the fractal dimension of the turbulent active region. Then we have

$$g(t) = 1 + \int_0^L dR\, h(R)(R/L_0)^{3\beta}\, F\{q(\varepsilon R)^{1/3} t(L_0/R)^{\beta}\}. \quad (2.20)$$

Clearly, $h(R)(R/L_0)^{3\beta}$ is the joint probability that a pair of particles separated by a distance R belongs to the same active region (a fractal) of turbulent flow, and $(\varepsilon R)^{1/3}(L_0/R)^{\beta}$ is the characteristic turbulent eddy velocity with intermittency corrections.

It should be noted that $g(t)$ is not assured of having scaling form $g(t) = g(x)$, where x is defined in eq. (1.1), merely because the characteristic function $F(y)$ in eq. (2.20) is of this form. However if $F(y)$ is an exponentially decaying function of its argument, and $h(R)$ in eq. (2.20) is an algebraic function of R, then it is indeed true that $g(t) = g(x)$, in accordance with our observations. We now examine the implication of the assumption that

$$F\{q(\varepsilon R)^{1/3} t(L_0/R)^{\beta}\} = F(y) \sim \exp(-y), \quad (2.21)$$

where $y = q(\varepsilon R)^{1/3} t(L_0/R)^{\beta}$. Inserting eq. (2.21) and eq. (2.11) into eq. (2.20) gives

$$g(x) = 1 + 2(L/L_0)^{3\beta} \exp(-x) \sum_{n=0}^{\infty} x^n \times (\Gamma\{3 + 9\beta)/(1 - 3\beta) + 1\})/((1 + 3\beta) \times \Gamma\{(3 + 9\beta)/(1 - 3\beta) + 1 + n\}) - \Gamma\{(6 + 9\beta)/(1 - 3\beta) + 1\}/((2 + 3\beta) \times \Gamma\{(6 + 9\beta)/(1 - 3\beta) + 1 + n\})). \quad (2.22)$$

Here x is defined in eq. (1.1) with $u(L) \sim (\varepsilon L)^{1/3}$, and $\Gamma\{z\}$ is

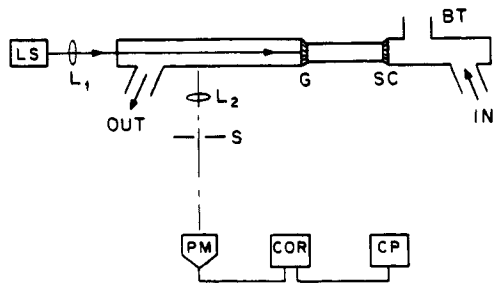

Fig. 1. Schematic diagram of the experimental setup. LS-Argon Ion Laser, L_1, L_2-Lenses, S-Slit, G-Grid, SC-Screen, BT-Air Bubble Trap, PM-Photomultiplier, COR-Correlator, CP-Computer, IN-Inlet of flow, OUT-Outlet of flow.

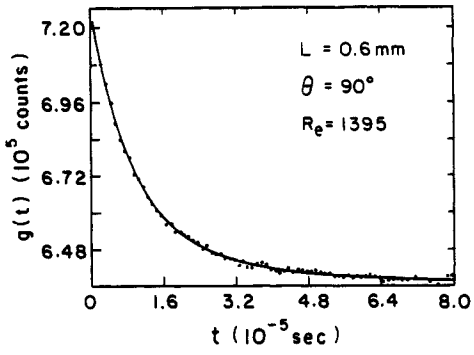

Fig. 2. A typical correlation function $g(t)$ vs. t. The solid curve is a fit to the Incomplete Gamma Function in eq. (2.23).

the Gamma Function. If $d = D$ ($\beta = 0$), eq. (2.22) becomes

$$g(x') = 1 + \exp(-x') \times \sum_{n=0}^{\infty} x'^n(12/(n+3)! - 720/(6+n)!). \quad (2.23)$$

where $x' = qu(L)t$. Note that the assumption of a single-exponential decay of $F(y)$ implies that $P(V(R)/u(R))$ is a Lorentzian function, for which all moments higher than the first diverge.

3. Experimental details

Figure 1 shows the physical arrangement of the experimental setup. The fluid, water, is circulated through a closed system by a pump. The water was seeded with polystyrene spheres of diameter 0.06 microns, the number density of polystyrene spheres being such that their mean spacing is much larger than their diameter (dilute solution) and much smaller than the smallest eddy size of the turbulent flow, L_d. This assures adequate sampling of the turbulent flow. A section of the pipe of 2.0 inch-diameter, is made of glass to admit the probing focused beam from an Argon-ion or He–Ne laser. Undesirable velocity fluctuations produced by the pump or by the pipe walls are damped out by a screen (SC) (aperture size = 2.0 mm) on the high-pressure side of the grid (G), which generated the turbulence. The spacing M between the grid rods was 3.1 mm and their diameter $d' = M/2$. The measuring point was on the axis of the pipe and 28 cm downstream from the grid ($x/M = 90$). The circulating fluid is temperature controlled. Ancillary LDV measurements established that the mean velocity profile was virtually flat rather than parabolic in the direction transverse to the mean flow direction when Re > 280, and that the turbulent intensity, $\langle v^2\rangle^{1/2}/U$, was 7% at Re = 700, where v is the fluctuation part of the mean velocity. These results suggest that the turbulence in our system did indeed originate from the grid, rather than from other sources.

The lens L_1 in Fig. 1 focuses the laser beam to make the scattering volume as one dimensional as possible on the axis of the pipe, while L_2 forms an image of this volume on the adjustable slit S, of width L. It is the light passing through the slit which illuminates the photomultiplier (PM). The water inlet and outlet as well as a stand-pipe (BT) where air bubbles can leave the fluid, are shown in Fig. 1. The output pulse train from the photodetector went to a commercial correlator (COR), whose output is $g(t)$. Also indicated is the computer (CP) for storing and analyzing the data.

The laser beam was sometimes brought into the fluid along the flow axis, as shown in the figure, but in other experiments where the direction of $\boldsymbol{q}$ was kept in parallel with the mean flow direction, it entered through the cylindrical glass pipe wall.

4. Results

The measured correlation functions were extremely well fitted to eq. (2.23) when 460 < Re < 1400, as may be seen in Fig. 2 (solid line), which shows $g(t)$ at Re = 1395, $q = 2.42 \times 10^5\ \mathrm{cm}^{-1}$ and $L = 0.6$ mm. Our experimental results could be fitted to eq. (2.23) only if x' is replaced by x of eq. (1.1) and let β be a function of Re. The fitting parameter $T'(x = t/T')$ exhibits the same slit width dependence as that of the half-decay time T of $g(t)$. Lacking a fully understanding of the functional form of $g(t)$ throughout the whole range of Re we have characterized $g(t)$ by its half-decay time T.

This fitting suggests that the velocity probability density function $P(V(R))$ has the scaling form of $P(V(R)/u(R))$ even though the flow falls far short of being fully developed. The fitting also indicates that the functional form of this scaling function $P(V(R)/u(R))$ is Lorentzian-like, at least for the most probable part of $P(V(R)/u(R))$ since $g(t)$ is relatively insensitive to the rare fluctuations of velocity. Our results of $P(V(R))$ are consistent with that obtained in strongly turbulent systems by Anselmet *et al.* [12]. They find that $P\{V(R)/u(R) > 2.0\}$ decays exponentially over five decades (P varies from 10^{-2} to 10^{-7}). However, the most probable part of $P(V(R)/u(R))$ ($P > 0.1$) is clearly not of exponential form, and indeed decays roughly as a Lorentzian function out to $V(R) \simeq 2u(R)$, where $u(R) = \langle V(R)^2\rangle^{1/2}$.

From the correlation function $g(t)$, we use eq. (1.2) to extract the interesting term $G(t) = (g(t)/\langle n\rangle^2 - 1)/f(L)$, which depends on control parameters U, q, and L. As Fig. 3 shows, $G(t)$ has the scaling form implied by eq. (2.23), i.e., $G(t)$ depends on these variables through the combination $G(t) = G(x)$, where x is given by eq. (1.1). The curves in Fig. 3 were obtained by first plotting $G(t)$ vs. t for different q and L with Re fixed. At each flow speed one obtains from these data curves of the shape seen in the figure. If now such a log–log plot is made at different Re, curves of the same shape are obtained, i.e. all such curves can be brought into coincidence merely by shifting the horizontal scales. Such scaling behavior is seen only if Re > 460. The data of Fig. 3 correspond to Re = 806 and 1364.

The analysis of our data, which yields Fig. 3, does not require knowledge of the scaling velocity $u(L)$. Hence no assumption was made for $u(L)$. Nevertheless, we do find that

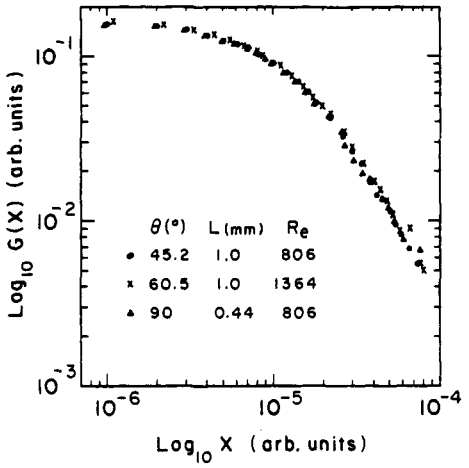

Fig. 3. The scaling function $G(x) = [\langle g(t)/\langle n\rangle^2\rangle - 1]/f(L)$ vs. $x = qu(L) \times t(L_0/L)^{\beta}$ at indicated parameters.

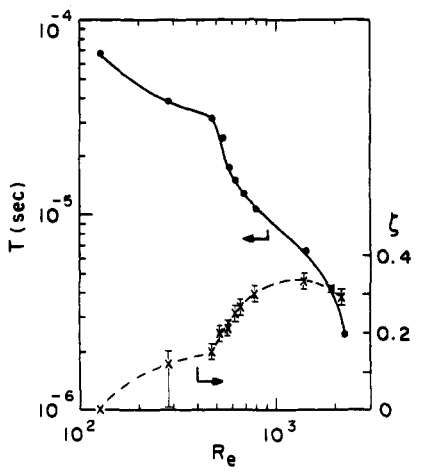

Fig. 5. The variation of the exponent $\zeta(x)$ and the logarithm of the half-decay time, log T(●), with the Reynolds number Re.

the function $u(L)$ which brings our data into scaling form, is roughly proportional to the control parameter U(U is proportional to Re). Therefore eq. (2.18) ($u(L) \sim L^{1/3}$) is taken as the definition of $u(L)$.

Figure 4 shows how T various with slit width L (in mm) at a fixed $q = 2.42 \times 10^5\,\mathrm{cm}^{-1}$ ($\theta = 90°$). The three curves correspond to Re = 460, 1400 and 2200. It is seen that increasing L reduces T in the range of 0.1 mm $< L <$ 1.0 mm. This is because opening up the slit increases the size of eddies seen by the photodetector, and larger eddies should have a shorter decay time. Using the Kolmogorov theory for a crude estimate of the decay time T, one gets, $T \sim 1/qu(L) \sim 1/q(\varepsilon L)^{1/3}$. The power-law behavior of T on L starts at $L =$ 1.0 mm which can be thought of as the outer scale of the turbulence generated by grid ($M = 3.1$ mm), i.e., $L_0 = 1.0$ mm.

Ideally T should be a constant when $L < L_d$ since there are no eddies smaller than L_d, and in fact one might hope to measure L_d($L_d \sim 0.01$ mm in our experiments) by finding the value of L at which T levels off as L is decreased. Unfortunately L_d could not be determined in this way because the diameter D' of the laser beam could not be reduced below 0.1 mm, and $D' \gg L_d$. Thus the turnover in $T(L)$ at small L was controlled by the laser beam diameter. In fact Fig. 4 reveals a decrease in T as L is reduced below the beam diameter, an effect which we do not understand. Focusing attention on the decade of slit widths, over which log (T) varies linearly with log (L) (see Fig. 4), we extract the slope ζ in the equation, $T \sim L^{-\zeta}$. If the scaling equations of Section 2 are correct, $\zeta = 1/3 - \beta$. It is seen that ζ does not vary with Re in a monotonic fashion. The numbers below each straight-line segment in Fig. 4 are the values of ζ at the three indicated Reynolds numbers.

Figure 5 shows more clearly the variation of ζ with Re (dashed curve, scale on right). Note the abrupt change in slope at Re = 460. This same kink is seen in the variation of T itself with Re (solid curve in Fig. 5, scale on left). These latter measurements were made at $L = 1.0$ mm. Here the incident laser beam entered the turbulent stream anti-parallel to the flow direction, and the scattering angle is 90°. Somewhat below Re = 460, the profile of the mean velocity, as determined by LDV, has become flat in the direction transverse to the pipe, i.e., the flow is plug-like, a phenomenon one associates with a turbulent state. Combining the discussions on Fig. 2 and Fig. 3. We therefore associate the abrupt slope change at Re = 460 with the onset of the turbulent velocity distribution having scaling character rather than a transition from laminar to turbulent flow.

The dashed curve in Fig. 5 also suggests a change in the character of the turbulence at higher Reynolds numbers. The exponent ζ rises to 0.33 ± 0.03 (the Kolmogorov value) at Re = 1400 and then decreases to 0.29 ± 0.03 at the maximum flow speed, which corresponds to Re = 2200. This drop in the exponent ζ is consistent with a smooth change from space-filling ($D = d$) to fractal ($D < d$) or intermittent turbulence, as seen in eq. (2.20). Intermittent turbulent flow is associated with the confinement of regions of high vorticity to very small regions of the fluid and is characterized by the fractal dimension D of the turbulent active region [19]. The decrease in ζ at large Re is unmistakable but very small. Only by going to higher flow speeds could one be sure that the effects is a real one.

Also measured was the q-dependence of the half-decay time T. Here the direction of $\boldsymbol{q}$ was held fixed, namely parallel to the flow direction, while its magnitude was varied. The slit width was fixed at $L = 1.0$ mm. To satisfy these conditions it is necessary to vary both the direction of the incident beam and the direction of the observation, which limited the range of q-values that could be spanned. It was found that $T(q)$ was also of power law form, $T \sim q^{-\mu}$. Our measurements of

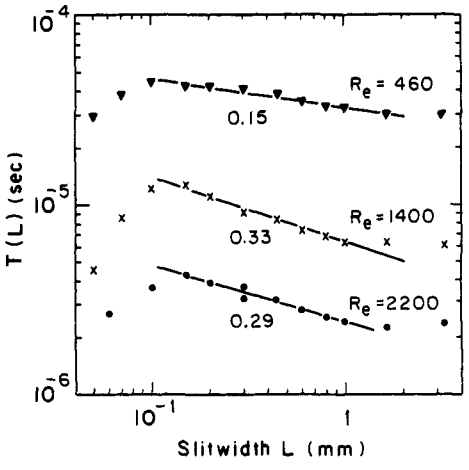

Fig. 4. The half-decay time T of $g(t)$ vs. slit width L at $q = 2.4 \times 10^5\,\mathrm{cm}^{-1}$. The number labeled below a line is the slope of that line.

Table I. *The variation of the exponent μ with the Reynolds number* Re *at* $L = 1.0$ mm

Re	0	125	280	460	775	1400	1860
μ	2.0	1.92	0.92	0.92	0.76	0.84	1.0

Note: Re = 0 is Brownian Motion, Re = 125 is laminar flow.

μ vs. Re are summarized in Table I, where μ is given for seven values of Re, from 0 to 1860. Note that when the flow is absent or laminar, the lifetime of the fluctuations is limited by the diffusive motion of the seed particles. In this case $T = 1/Dq^2$, where D is the Stokes law diffusivity of a Brownian particle. As the value of Re increases, the exponent μ falls below 1.0 from 2.0 and then increases toward 1.0, a value which was obtained at Re = 1860. Thus $\nu = 1$ is chosen for the scaling form of $G(x)$, where x is defined in eq. (1.1).

5. Summary

We have studied the small-scale grid-generated turbulence with the rarely exploited technique of photon correlation spectroscopy. Measurements of this type give access to the probability density $P(V(R))$ that a pair of particles in the fluid, having separation R, differ in velocity by $V(R, t)$. At moderate Reynolds number the intensity correlation function $g(t)$ has the scaling form $g(x)$, where $x = qu(L)t(L_0/L)^{\beta}$, $u(L) \sim \varepsilon L)^{1/3}$ is the characteristic turbulent velocity, and $\beta = \beta(\mathrm{Re})$. This scaling behavior is seen only if Re > 460. All the measurements suggest that the flow changes its character at this point. In this experiment the exponent β should probably not be regarded as a measure of the intermittency. Rather it may be seen as an additional Reynolds number dependent parameter that is needed to characterize the flow at moderate turbulent levels. The experimental technique used here is most sensitive to the most probable part of $P(V(R))$ and hence to small values of $V(R, t)$. In this range our results are consistent with a Lorentzian form for $P(V(R)/u(R))$ or, equivalently an exponential decay for its characteristic function $F(x)$. This finding is a consistent with those obtained by Anselmet *et al.* [12], though the values of Re achieved in the present experiment are much smaller than theirs.

Acknowledgements

This work is collaboration of C. K. Chan and A. Sirivat, in addition to the authors of this paper. The four of us are indebted to J. Stavans for simulating comments and especially to A. Onuki for the insights he has provided. In its early stages, this research received valuable stimuli from I. Procaccia. Our work is supported by the National Science Foundation under grant DMR-8611666.

References

1. Drain, L. E., The Laser Doppler Technique. John Wiley & Sons (1980).
2. Durst, F., *et al.*, Principles & Practice of Laser-Doppler Anemometry, 2nd Ed. Academic Press (1981).
3. Buchhave, P., George, W. K. Jr., and Lumley, J. L., the Measurement of Turbulence with the Laser-Doppler Anemometer, in Annual Review of Fluid Mechanics, **11**, 443 (1979).
4. Bourke, P. J., *et al.*, J. Phys. A: Gen. Phys. **3**, 216 (1970).
5. Smol'yakov, A. V., & Tkachenko, V. M., the Measurement of Turbulent Fluctuations, Eng. Ed. Springer-Verlag (1983).
6. Lumley, J. L., Phys. Fluids, **8**, 1056 (1965).
7. Berne, B. J. and Pecora, R., Dynamic Light Scattering. John Wiley & Sons (1976).
8. Frisch, U., Sulem, P., and Nelkin, M., J. Fluid. Mech. **87**, 719 (1978).
9. Van Atta, C. W. and Park, J., Statistical self-similarity and inertial subrange turbulence, in Statistical Models and Turbulence, Rosenbblatt, M. & Van Atta, C. W., Eds., Lectures Notes in Physics, **12**, 402 (Springer 1972).
10. Rose, H. A. and Sulem, P. L., J. de Physique **39**, 443 (1978).
11. Dutton, J. A. and Deaven, D. G., Radio Science **4**, 1341 (1969).
12. Anselmet, F., *et al.*, J. Fluid Mech. **140**, 63 (1984).
13. Antonia, R. A., Satyprkash, B. R., and Hussain, A. K., Phys. Fluids **25**, 29 (1982).
14. Schuster, H. G., Deterministic Chaos (Physik-Verlag 1984).
15. Gibson, C. H. and Schwarz, W. H., J. Fluid Mech. **16**, 364 (1963).
16. Kolmogorov, A. N., C. R. Acad Sci. U.S.S.R. **30**, **301**, 538 (1941).
17. Chan, C. K., *et al.*, to be published. In general one cannot factor $g(t)$ into spatial- and time-dependent parts, though this factorization is exact if the source of the scattering has a Gaussian distribution.
18. In eq. (2.10) (and hereafter) we have ignored the fact that the integral over R has a lower cut-off, L_d. This approximation is valid when $L_d/L \ll 1$, i.e., we have assumed that a small fraction of the integral in eq. (2.10) comes from the interval $0 < R < L_d$.
19. Hentschel, H. E. and Procaccia, I., Phys. Rev. Lett. **49**, 1158 (1982).